Military Technical College
Kobry El-Kobbah,
Cairo, Egypt.

13th International Conference on Applied Mechanics and Mechanical Engineering.

SIMULATION OF ACOUSTIC GENERATION AND PROGRESSION IN A CLOSED CHAMBER

MOHD-GHAZALI[1] N. and McHUGH[2] J.P.

ABSTRACT

Theoretical and experimental studies in thermoacoustics successfully explained the phenomena with linear inviscid theory at lower oscillation amplitudes. The theory is inadequate at higher oscillations because of dominant nonlinear and multidimensional effects. This study is part of a research into the simulation of the nonlinear behavior of fluid in an acoustic chamber at near incompressible flow. A time-dependent compressible Navier-Stokes system was solved for a two-dimensional rectangular chamber with a membrane and a closed end on the other. The generation and progression of the simulated velocity field observed is significantly complex which include beatings, vortex motions, and cross-waves, among others. Computations have shown vortex shedding behavior near the membrane acoustic driver as well as near heat exchanging plates when they are included for both pure Helium and mixtures. Simulations also showed acoustic streaming, a secondary flow forced by the acoustic waves. Quantitatively small, the streaming flow increases steadily with time. The paper reports the simulation results obtained. These complexities have only been previously reported independently and to date many open questions still remain on some issues.

KEY WORDS

Thermoacoustics, simulation, cross-waves, streaming, vortex shedding

---

[1] Faculty of Mechanical Engineering, University Teknologi Malaysia, Malaysia
FAX: 07-5566159, E-mail: normah@fkm.utm.my

[2] Department of Mechanical Engineering, University of New Hampshire, Durham, NH 03824, USA.

INTRODUCTION

The field of thermoacoustics basically involves the interaction of acoustic waves and solid boundaries. Expansion and compression of fluid particles in acoustic waves are generally followed by temperature oscillations. These oscillations of fluid particles when in contact with solid boundaries can generate powerful and useful thermodynamic effects - acoustic power. Sound waves encountered in our daily life produce this same effect but the order of magnitude is generally too small to be noticed. The phenomena can be classified into (i) a temperature gradient-induced oscillations and (ii) temperature gradient induced by oscillations. The first is found in a thermoacoustic heat engine, a prime mover that operates as that taught in an introductory thermodynamics course. Power is generated in the form of acoustic waves as heat is transferred from a high-temperature reservoir to a low-temperature reservoir. This is achieved through a temperature gradient across heat exchanging plates within a stack that is externally connected to the heat reservoirs. The flow of heat and work is reversed in the thermoacoustic heat pump or refrigerator. Work input in the form of acoustic waves generates a temperature gradient across the stack as transfer of heat from a low-temperature to a high-temperature reservoir occurs.

Thermoacoustic phenomena was actually first observed by European glass blowers about 200 years ago, when sound is sometimes heard when a hot glass bulb is attached to a cool glass tubular stem. The first qualitative discussion of the temperature-gradient induced oscillations was done in 1896 which can be found in Lord Rayleigh's *The Theory of Sound* [1]. Accurate qualitative discussions are only achieved over 150 years later by Nicholas Rott [2]. Studies into its practical application, however, did not start until in the mid eighties. Much experimental and theoretical work has been done since to better understand the thermodynamics behind the phenomena, references [3-7] are some of them.

Less is known about the temperature gradient that is induced by oscillations than about oscillation-induced temperature gradient. Merkli and Thomann presented the theory behind the slight cooling of a resonating gas in a chamber in 1975 [8]. A test-bed cryocooler made by Hofler was probably the first practical thermoacoustic refrigerator [9]. It was a gas-filled resonator containing a stack of plates and driven by a loudspeaker. Thermoacoustic refrigeration system is an attractive replacement to the current system because of its simplicity and environmentally friendly operation.

The numerical results given herein treat the entire resonator, and allow the acoustic wave to evolve in time, adjusting to the no-slip boundary conditions. Analytical solution is strictly limited to 1-dimension and numerical work so far has concentrated on the heat-exchanging stack region [10-13]. Worlikar and Knio used central differencing on rectangular grids. The Navier-Stokes system is solved implicitly to first order. Their numerical study, however, covers only the region enclosing two plates and without any oscillating flow anywhere in their computational domain. They also neglect thermal diffusion. Cao et.al also modified the two plate region using finite differencing, discretized the governing equations on staggered grids. Their numerical method was only first order accurate in time, and the physical model included both the diffusive and dissipative effects. However, the boundary conditions have assumed a priori the presence of standing wave and/or travelling wave on the left and right side of the horizontal plates. Tang etc. el modeled a thermoacoustic resonator with linear thermoacoustics system of equations, also assuming the establishment of a standing

wave in the simulation [14]. The present simulation treats the entire resonator, and allows the acoustic wave to evolve in time, adjusting to the no-slip boundary conditions, the presence of heat exchanging plates, and other features.

NUMERICAL FORMULATION

The governing equations are the unsteady two-dimensional equations of continuity, momentum, and energy, assuming a compressible Newtonian fluid with constant thermophysical properties. Ideal gas behavior is assumed for the working fluid in the chamber. Separating the variables pressure, velocities, and the temperature into its mean and fluctuating parts,

$$p = p_m + p', \tag{1}$$

$$u = u_m + u', \tag{2}$$

$$T = T_m + T', \tag{3}$$

the Navier-Stokes system of equations are non-dimensionalized using the height of the resonator, H, and the circular frequency of the acoustic waves, ω. The resulting dimensionless system of equations in Cartesian coordinates for two-dimensions is

$$\frac{\partial^2 u}{\partial t^2} = \frac{1}{Ma^2\gamma}\left(\frac{\partial^2 u}{\partial x^2} + \frac{\partial^2 v}{\partial x \partial y} - \frac{\partial^2 T}{\partial x \partial t}\right) + \frac{1}{\mathrm{Re}}\frac{\partial}{\partial t}(\nabla^2 u) + \frac{1}{3\,\mathrm{Re}}\frac{\partial}{\partial t}\left(\frac{\partial^2 u}{\partial x^2} + \frac{\partial^2 v}{\partial x \partial y}\right) + \frac{1}{Ma^2\gamma}\frac{\partial}{\partial x}(Q_p) - \frac{\partial}{\partial t}(Q_x), \tag{4}$$

$$\frac{\partial^2 v}{\partial t^2} = \frac{1}{Ma^2\gamma}\left(\frac{\partial^2 u}{\partial x \partial y} + \frac{\partial^2 v}{\partial y^2} - \frac{\partial^2 T}{\partial y \partial t}\right) + \frac{1}{\mathrm{Re}}\frac{\partial}{\partial t}(\nabla^2 v) + \frac{1}{3\,\mathrm{Re}}\frac{\partial}{\partial t}\left(\frac{\partial^2 u}{\partial x \partial y} + \frac{\partial^2 v}{\partial y^2}\right) + \frac{1}{Ma^2\gamma}\frac{\partial}{\partial x}(Q_p) - \frac{\partial}{\partial t}(Q_y), \tag{5}$$

$$\frac{\partial T}{\partial t} = \frac{\gamma}{Pe}\nabla^2 T + (1-\gamma)(\nabla \cdot u) + (1-\gamma)Q_p - \gamma Q_T, \tag{6}$$

$$\frac{\partial p}{\partial t} = \frac{\gamma}{\gamma - 1}\left(\frac{\partial T}{\partial t} - \frac{1}{Pe}\nabla^2 T + Q_T\right), \tag{7}$$

where the subscripted Q's are the non-linear terms.Bulk viscosity is assumed to be zero, and body forces have been excluded. Three dimensionless groups of parameters are introduced in the non-dimensionalizing process, the Reynolds number, Re; the Peclet number, Pe; and the Mach number, Ma.

$$\mathrm{Re} = \frac{H^2\omega}{\nu}, \tag{8}$$

$$Pe = \frac{H^2 \omega}{\alpha}, \tag{9}$$

$$Ma = \frac{H\omega}{\sqrt{\gamma RT}}, \tag{10}$$

where ν is the kinematic viscosity, α the thermal conductivity, and γ the ratio of specific heats of the fluid. The boundary conditions are the no-slip, no-penetration, and zero heat flux on the walls. The fluctuating quantities are set to zero at t=0. The spatial derivatives are approximated with finite differences, accurate to second order. Interior grid points use central differences and one-sided derivatives are used on the boundaries [14],

The temporal integration is achieved with a semi-implicit method, where linear terms are treated implicitly, and the non-linear terms explicitly. The linear terms in the equations containing first order temporal derivatives are treated with the Crank-Nicholson method in the usual manner. The non-linear terms are treated with the Adams-Bashforth method. This procedure produces no artificial damping of the acoustic waves as is found in methods where the pressure and velocity terms are coupled. Waves are then forced by imposing the normal component of velocity along one side of the wall, as in a membrane acoustic driver,

$$u(0,y) = u_0 \sin(y) \sin(t), \tag{11}$$

where u_0 is the dimensionless forcing amplitude of the velocity. The computational formulation has been verified against available theoretical solutions [15]. When a solid plate is in position, equations (4)-(7) are solved simultaneously with the dimensionless energy equation for the solid,

$$\frac{\partial T_s}{\partial t} = \frac{1}{Pe_s} \nabla^2 T_s, \tag{12}$$

where T_s is the temperature of the solid plate material, and

$$Pe_s = \frac{h^2 \omega}{\alpha_s}, \tag{13}$$

h being the thickness of the plate, and α the thermal diffusivity of the plate material. The thermal properties of the plate material are assumed to remain constant, and are chosen to model stainless steel (type 304). The plate employs the same computational grid as the fluid, which is uniform in both directions. Hence the plate boundaries correspond exactly to grid points in the fluid.

RESULTS AND DISCUSSION

Based on a set of parameters (shown in table 1) for the simulation, the forcing is maintained for the duration of the simulation.

Table 1. Parameters used in the simulation

Pm	101 kPa
Tm	293K
Ma	0.7854
Re	800000
Pe	600000
Δt	0.001
Δx	0.01

The Mach number is chosen so that the forcing will produce waves with a half wavelength that matches the resonator length. The resonator has an aspect ratio, L/H, of 4 with the membrane forcing amplitude of velocity at 0.001. The value of Pe_s is 2.247 x 10^7 calculated for stainless steel plate. The desired result of the forcing is a standing acoustic wave. However, the time-dependent results show that the velocity field is significantly more complex than the expected standing wave. Beating phenomena, cross waves, streaming, oscillatory boundary layers and vortex motion are observed [15]. Figure 1 shows the region where the vector plots of Fig. 2 and 3 are shown.

The vortex also appear at the top right-hand corner of the chamber but is absent at the corners near the end wall. The vortex shed itself with time, appearing again in the next cycle. Vortices also appear next to the stack/heat exchanging plates when they are located within the chamber [15]. Several studies have been completed since the behavior was first reported, probably at the First Thermoacoustic Workshop held in Netherlands in April of 2001. Figure 4 and Figure 5 show other complexities observed in the simulation. Figure 4 shows the development of cross-waves, waves appearing at right angle to the incident waves, as the simulation is completed for ten cycles, and Figure 5 shows the total kinetic energy, $\overline{KE}$. It can be seen that the amplitude of oscillation has its own oscillation believed to have been caused by two incommensurate frequencies which are close in value.

There have been isolated reports on these complexities before; Atchley [3] and Keolian [16] found beatings or sub-harmonic oscillations in experiments with acoustic resonators; vortex shedding behavior was observed numerically by Worlikar and Knio [10], and experimentally by Wetzel and Herman [17]. Vortices were also recorded in a numerical simulation of mixed gases; He-Ar, He-Ne and He-Xe under similar operating conditions [18]. Cross-wave profiles were reported by Aranha et. al. [19] and acoustic streaming was briefly discussed in Rayleigh's volumes, The Theory of Sound [1]. Acoustic streaming, a second-order flow driven by the first-order acoustic oscillations is believed to cause heat leaks in high-power operating regimes of thermoacoustic devices [20]. Significant progress in the studies of the complex behavior has been achieved to date but many open questions still remain. The complex behavior mentioned has been simultaneously observed in this simulation completed in 2001 for pure Helium with some similar behavior also recorded in an extended study for mixtures by the author in 2006 [18]. Follow ups are made difficult due to the huge gap between the particle velocity and wave speed, and the large computational domain to be covered for a thermoacoustic resonator. Steady-state condition where a standing wave is desired cannot be observed after several cycles of acoustic generation. The

observed behavior of the generation and progression of acoustic waves, however, has shown that waves in the thermoacoustic resonator behave similarly as normal waves under similar circumstances but more studies need to be done to determine the extend of these effects when the standing wave is finally established. Numerical simulation may lead researchers to understand the effects that dimensionality and nonlinearities have on the performance of the systems, what analytical and experimental approaches have failed to do so far under normal operating regimes.

CONCLUSIONS

Simulation of acoustic waves in a thermoacoustic resonator with a membrane acoustic driver shows the presence of complexities that have been reported independently. It may be assumed that the same theories that apply to each phenomenon are also an integral part of the behavior observed as acoustics are generated and progressed in this time-dependent nonlinear numerical simulation. To date, although many successful thermoacoustic systems have been produced, many open questions still remain which require further investigations into the effects of dimensions and nonlinearities on the performance of a thermoacoustic system. The author is currently pursuing simulation into mass diffusion between the heat exchanging plates that follows the oscillation of acoustic waves.

ACKNOWLEDGEMENTS

The authors would like to thank Universiti Teknologi Malaysia (UTM) and the Ministry of Science and Technology (MOSTI) of Malaysia for their financial assistance to this research.

REFERENCES

[1] Strutt, J.W., The Theory of Sound, Academic Press, Vol. I, (1945).
[2] Rott, N., Thermoacoustics, Adv. Appl. Mech. 20, 135 (1980).
[3] Atchley, A.A., Hofler, T.J., Muzzerall, M.L., Kite, D., and Ao, C., Acoustically Generated Temperature Gradients in Short Plates, J. Acoust. Soc. Am. 88(1), 251-263 (1990).
[4] Garrett, S.L., Adeff, J.A., and Hofler, T.J., Thermoacoustic Refrigerator for Space Applications, J. of Thermophysics and Heat Transfer, 7, 595-599 (1993).
[5] Yuan, H., Karpov, S., and Prosperetti, A., A Simplified Model for Linear and Nonlinear Processes in Thermoacoustic Prime Movers. Part II. Nonlinear Oscillations, J. Acoust. Soc. Am. 102(6), 3497-3506 (1997)
[6] Wakeland, R.S. and Keolian, R., Thermoacoustics with Idealized Heat Exchangers and No Stack, J. Acoust. Soc. Am., 111 (6), 2654-2664 (2002).
[7] Aktas, M.K., Thermoacoustically Induced and Acoustically Driven Flows and Heat Transfer in Enclosures, Ph.D. dissertation Drexel University, USA (2004).
[8] Hofler, T.J., Thermoacoustic Refrigerator Design and Performance, Ph.D. dissertation, Physics Dept., Univ. of California at San Diego (1986).
[9] Merkli, P., and Thomann, H., Thermoacoustic Effects in a Resonance Tube, J.

Fluid Mech. 70, 161-177 (1975).
[10] Worlikar, A.S., and Knio, O.M., Numerical Simulation of a Thermoacoustic Refrigerator, J. Computational Physics 127, 424-451 (1996).
[11] Cao, N., Olson, J.R., Swift, G.W., and Chen, S., Energy Flux Density in a Thermoacoustic Couple, J. Acoust. Soc. Am. 99(6), 3456-3464 (1996).
[12] Gopinath, A., Tait, N.L., and Garrett, S.L., Thermoacoustic Streaming in a Resonant Channel: The Time-Averaged Temperature Distribution, J. Acoust. Soc. Am. 103(3), 1388-1404 (1998).
[13] Herman, C., and Chen, Y., A Simplified Model of Heat Transfer in Heat Exchangers and Stack Plates of Thermoacoustic Refrigerators, Heat Mass Transfer, Springer-Verlag On-Line, 901-917 (2006).
[14] Tang, K., Chen, G.B., Jin, T., Bao, R., Kong, B., and Qiu, L.M., Influence of Resonance Tube Length on Performance of Thermoacoustically Driven Pulse Tube Refrigerator, Cryogenics 45, 185-191 (2005).
[15] Anderson, D.A., Tannerhill, J.C., and Pletcher, R.H., Computational Fluid Mechanics and Heat Transfer, Taylor & Francis (1984).
[16] Mohd.Ghazali, N., Numerical Simulation of Acoustic Waves in a Rectangular Chamber, Ph.D. dissertation, Univ. of New Hampshire, USA (2001).
[17] Keolian, R., Turkevich, L.A., Putterman, S.J., Rudnick, I., and Rudnick, J.A., Subharmonic Sequences in the Faraday Experiment: Departures from Period Doubling, Physical Review Letters 47(16) 1133-1136 (1981).
[18] Wetzel, A.S. and Herman, C., Design Issues of a Thermoacoustic Refrigerator and its Heat Exchangers, HTD-Vol 331, National Heat Transfer Conference, Vol 9. ASME 137-144.
[19] Aranha, J.A., Yue, D.K.P., and Mei, C.C., Nonlinear Waves Near a Cut-Off Frequency in an Acoustic Duct – A Numerical Study, J. Fluid Mech. 121, 465-485 (1982).
[20] Matveev, K., Backhaus, S., and Swift, G., On Some Nonlinear Effects of Heat Transport in Thermal Buffer Tubes, 17th International Symposium on Nonlinear Acoustics, State College, PA USA (2005).

Fig. 1. Schematic of entire chamber showing vector plot region

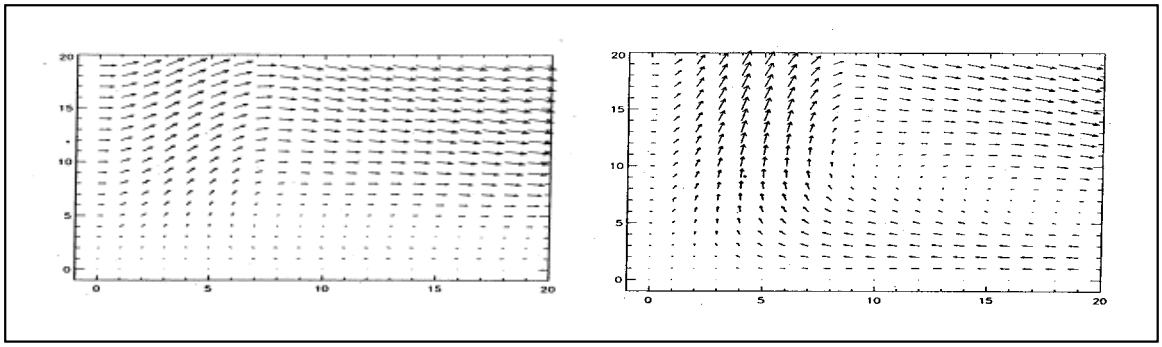

Fig. 2. Vector plot near bottom corner at (a) t = 2.701, (b) t = 3.001

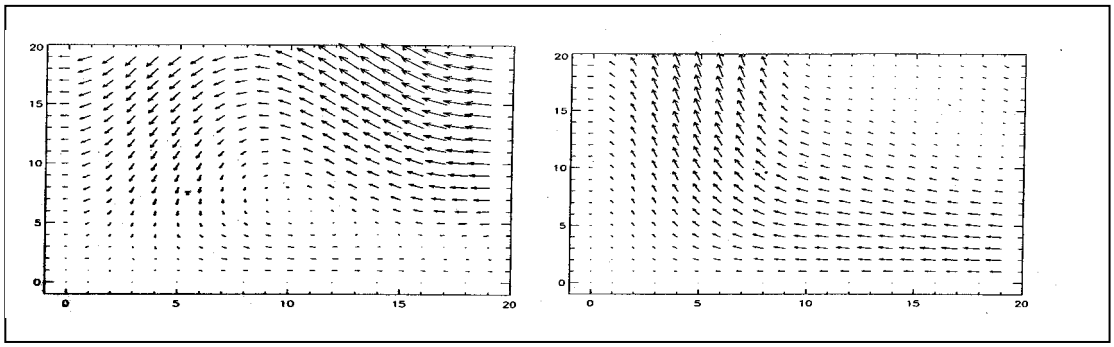

Fig. 3. Vector plot near bottom corner at (a) t = 3.301, (b) t = 6.001

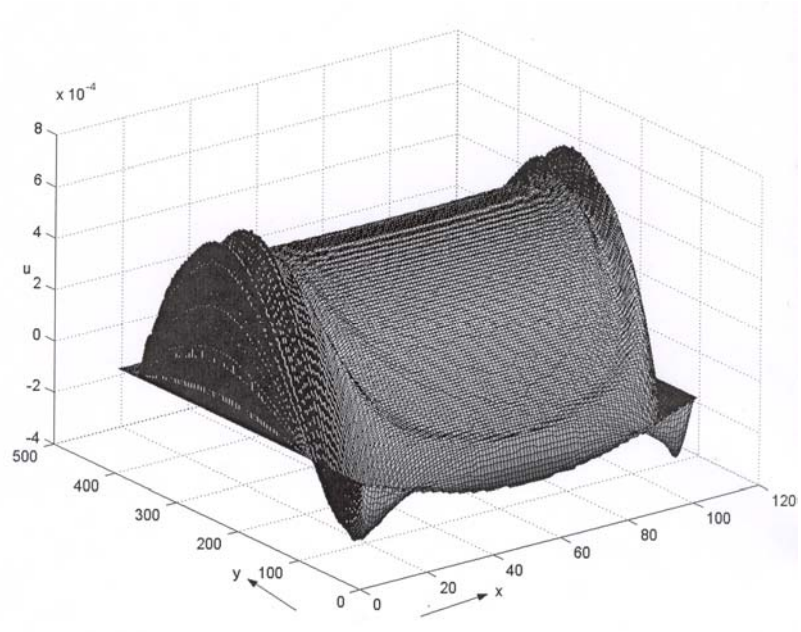

Fig. 4. Acoustic wave with developing cross-waves.